Complex periodic orbits, renormalization, and scaling for quasiperiodic golden-mean transition to chaos

Nikolai Yu. Ivankov[1] and Sergey P. Kuznetsov[2]
[1]*Saratov State University, Astrakhanskaja 83, Saratov, 410026, Russian Federation*
[2]*Institute of Radio-Engineering and Electronics RAS, Saratov Division, Zelenaya 38, Saratov, 410019, Russian Federation*
(Received 30 March 2000; revised manuscript received 8 November 2000; published 28 March 2001)

At the critical point of the golden-mean quasiperiodic transition to chaos we show the presence of an infinite sequence of unstable orbits in complex domain with periods given by the Fibonacci numbers. The Floquet eigenvalues (multipliers) are found to converge fast to a universal complex constant. We explain this result on the basis of the renormalization group approach and suggest using it for accurate estimates of the location of the golden-mean critical points in parameter space for a class of nonlinear dissipative systems defined analytically. As an example, we obtain data for the golden-mean critical point in the two-dimensional dissipative invertible map of Zaslavsky. We give a set of graphical illustrations for the scaling properties and emphasize that demonstration of self-similarity on two-dimensional diagrams of Arnold tongues requires the use of a properly chosen curvilinear coordinate system. We discuss a procedure of construction of the appropriate local coordinate system in the parameter plane and present the corresponding data for the circle map and Zaslavsky map.

DOI: 10.1103/PhysRevE.63.046210 PACS number(s): 05.45.Df, 05.10.Cc

I. INTRODUCTION

Very often the creation of several oscillatory components comes before the transition to chaos in multidimensional nonlinear systems. The frequencies of these components normally depend on control parameters. If the frequency ratios f_i/f_j are irrational, the attractor is a torus of dimension determined by the number of relevant oscillatory motions. When the values of f_i/f_j become close to rational numbers, the oscillations show a tendency to mutual synchronization (mode locking) accompanied by formation of an attractor that is a lower dimensional torus or a periodic orbit. Quasiperiodic and periodic regimes can undergo further bifurcations, which may finally lead to chaos. This picture is referred to as the route to chaos via quasiperiodicity. Starting from seminal works of Landau [1] and Ruelle and Takens [2], numerous studies have been devoted to different aspects of this picture [3–29].

Let us take a two-dimensional torus and tune the parameters of the dynamical system to keep fixed the irrational frequency ratio of two excited oscillatory components and avoid mode locking. In the parameter space this corresponds to a path along a definite curve. This curve may be terminated by a critical point separating quasiperiodic and chaotic regimes. For a detailed investigation of such a transition it is common to choose the golden-mean frequency ratio $f_1/f_2 = \omega = (\sqrt{5}-1)/2$. The rational approximants for this ω are represented by ratios of Fibonacci numbers, $\omega_m = F_{m-1}/F_m$, where $F_0=0, F_1=1, F_{m+1}=F_m+F_{m-1}$. It is convenient to deal with the golden mean because of the simplicity of the theoretical analysis. Another reason follows from the fact that this irrational number is characterized by the slowest convergence of the sequence of rational approximants. Due to this, the fine structure of the parameter space near the golden-mean frequency ratio in experiments and computations appears to be more distinguishable than at other irrational ratios.

The simplest model in which the discussed transition occurs is the one-dimensional circle map

$$\theta_{n+1} = \theta_n + \Omega - (k/2\pi)\sin 2\pi\theta_n . \tag{1}$$

Here θ is the dynamical variable, n is discrete time, and Ω and k are parameters. The winding number $w = \lim_{n\to\infty} \theta_n/n$ plays the role of the frequency ratio. The variable θ is interpreted as a kind of phase (only the fractional part of θ is of relevance), so regimes with rational winding numbers are regarded as periodic.

In Fig. 1(a) we present a chart of the parameter plane (k,Ω). Regions of different dynamical behavior are shown in gray scale. Domains of synchronization, known as Arnold tongues, correspond to rational winding numbers. The horizontal line $k=1$ separates two essentially distinct parts of the parameter space: below this line the map is invertible, above this line it is not. At $k<1$ quasiperiodic regimes occur between the tongues.

In the parameter plane one can find a curve $\Omega = \Omega_\omega(k)$ of constant irrational winding number $w=\omega=(\sqrt{5}-1)/2$ [Fig. 1(b)]. Just on the border of the invertibility loss this curve terminates at the point

$$(k_c, \Omega_c) = (1, 0.606\,661\,063\,470\,185\ldots), \tag{2}$$

which will be referred to as *the GM critical point* (GM stands for ''golden mean''). Scaling properties intrinsic to this point were discovered in numerical computations by Shenker [3]. The theoretical foundations were stated by Feigenbaum, Kadanoff, and Shenker [4], and by Rand, Ostlund, Sethna, and Siggia [5,6]. They developed the renormalization group (RG) approach based on constructing a sequence of evolution operators—maps describing the dynamics in terms of properly rescaled variables over time

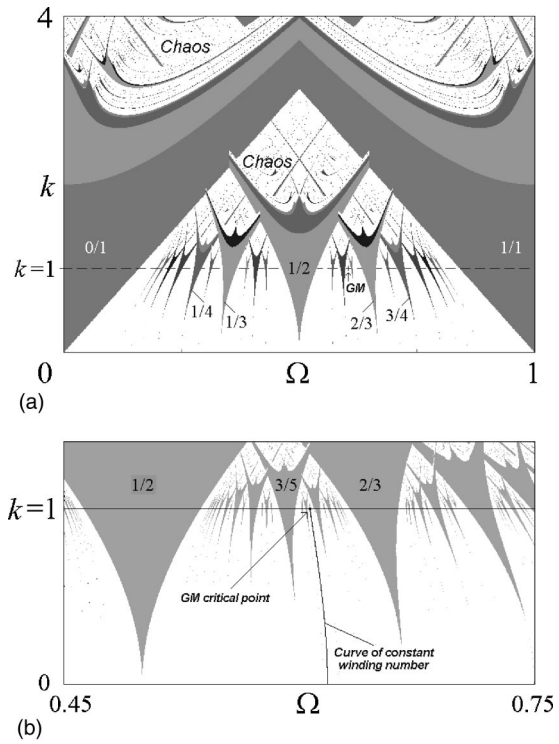

FIG. 1. (a) Parameter plane of the circle map (1). Regions of synchronization (Arnold tongues) are shown in gray; winding numbers are indicated inside the tongues. White regions correspond to quasiperiodicity (below $k=1$), chaos (above $k=1$), or unrecognized long periods. (b) Illustration of the GM critical point definition: in the parameter plane this is a terminal point of the curve of constant irrational winding number $(\sqrt{5}-1)/2$ located at the border of invertibility loss. In the diagram (a) the critical point is marked by a small cross.

intervals given by the Fibonacci numbers. From the RG analysis the constants were obtained [3–6,28,29] responsible for scaling in the phase space

$$\alpha = -1.288\,574\,553\,954\,368\,866\ldots \tag{3}$$

and in the parameter space

$$\delta_1 = -2.833\,610\,655\,891\,167\,799\ldots,$$

$$\delta_2 = \alpha^2 = 1.660\,424\,381\,098\,700\,680\ldots. \tag{4}$$

It is commonly believed that a critical point of the same kind occurs in nonlinear dissipative systems of different natures. This assertion is supported by some experimental and numerical studies, including experiments on Rayleigh-Bénard convection [9,13,14,17,25].

As known, the simplest class of continuous time systems possessing complex dynamics and chaos is represented by three-dimensional flows. Using construction of the Poincaré section, one can reduce the description of the dynamics to a two-dimensional invertible map. In the parameter space of such a system the terminal point of a curve of constant winding number cannot be associated with violation of the invertibility. So the question arises of how one can find the critical point in this case. Some ways to solve this problem have been discussed in the literature [23–25], but we intend to present here an alternative approach.

To invent an algorithm for computation of the critical point we recall a similar problem for the period doubling transition to chaos. In that case an elegant method is known based on so-called eigenvalue matching [30–33]. At the Feigenbaum critical point an infinite set of unstable periodic orbits is present. Periods are equal to 2^m, and cycle eigenvalues (multipliers) converge to a universal constant $\mu_c = -1.601\,19\ldots$. The value of the control parameter is selected to reach equality of the multipliers for two sufficiently long periods, and it yields a good estimate for the critical point. Alternatively, one can search for the parameter value at which the multiplier for one period 2^m equals μ_c. The larger m is, the more precisely the value of the parameter will be obtained. An analogous approach was exploited in studies of the destruction of ''noble'' Kolmogorov-Arnold-Moser tori in Hamiltonian dynamics [35–38]. In particular, for the golden-mean frequency ratio there exists an infinite set of unstable orbits with periods given by Fibonacci numbers. Their eigenvalues are expressed via the so-called residue, which tends to a universal constant.

In the dissipative case no periodic orbits occur at the GM critical point. Nevertheless, as we show in the present paper, a set of orbits with desirable properties does exist in the complex domain of the dynamical variables. Hence, application of a similar method for computation of the GM critical point becomes possible. As a basic example, we take a popular two-dimensional invertible map, which has been derived from realistic physical assumptions—the standard dissipative map of Zaslavsky [9,25,35].

Having found accurately the critical point GM for this map we will discuss in some detail the intrinsic scaling properties, which are common for all representatives of the universality class including the one-dimensional circle map [3–9,16,19,20,28,29]. In particular, we pay special attention to the self-similar arrangement of the picture of Arnold tongues near the GM critical point. To our knowledge, no convincing illustrations of two-dimensional scaling have been presented in the literature, even for the circle map. Apparently, the reason is a subtlety of the question: as we argue, some special nonlinear coordinate change must be implemented to define in the parameter plane a coordinate system appropriate for demonstration of the scaling property. Without properly chosen local coordinates no perfect correspondence of the parameter space arrangement on different scales can be observed (see, e.g., [34]).

In Sec. II we present numerical evidence that the circle map at the GM critical point possesses an infinite sequence of orbits (cycles) in the complex domain with periods given by Fibonacci numbers and with Floquet eigenvalues (multipliers) converging to a universal complex constant. In Sec. III we briefly reproduce the RG analysis for a one-dimensional map and use it to explain the results of the previous section. In particular, the value of the universal multiplier is obtained from the solution of the RG equation. In Sec. IV we formulate a method of precise computation of the critical point. It consists in selecting appropriate values of

TABLE I. Complex cycles and their multipliers at the GM critical point of the circle map (1): $k=1$, $\Omega=0.606\,661\,063\,470\,185$.

Period	θ_0	μ
5	$0.116329865+0.107284031i$	$0.744652+2.595925i$
8	$-0.092281354-0.082307114i$	$0.746874+2.519519i$
13	$0.071212941+0.063688363i$	$0.741626+2.556631i$
21	$-0.055637081-0.049219831i$	$0.742948+2.536090i$
34	$0.043111983+0.038153899i$	$0.741842+2.546574i$
55	$-0.033526721-0.029566354i$	$0.742304+2.540931i$
89	$0.026008785+0.022934662i$	$0.742035+2.543873i$
144	$-0.020197246-0.017789510i$	$0.742174+2.542310i$
233	$0.015672853+0.013803118i$	$0.742103+2.543132i$
377	$-0.012165420-0.010710054i$	$0.742143+2.542697i$
610	$0.009440876+0.008310980i$	$0.742123+2.542927i$
987	$-0.007327078-0.006449351i$	$0.742134+2.542804i$
1597	$0.005686194+0.005004901i$	$0.742128+2.542873i$
2584	$-0.004412866-0.003883963i$	$0.742134+2.542825i$

control parameters to reach the universal value of the multiplier for a complex orbit of period given by a sufficiently large Fibonacci number. The method is applied to the Zaslavsky map, and the GM critical point is found. In Secs. V and VI we discuss and compare the scaling properties of the Zaslavsky map and the circle map at the GM point and in its neighborhood.

II. COMPLEX PERIODIC ORBITS OF THE CIRCLE MAP

Let us suppose that the dynamical variable in the circle map (1) is complex, although the parameters Ω and k remain real. The substitution $\theta_n=x_n+iy_n$ and separation of real and imaginary parts yields

$$x_{n+1}=x_n+\Omega-(k/2\pi)\cosh 2\pi y_n \sin 2\pi x_n,$$

$$y_{n+1}=y_n-(k/2\pi)\sinh 2\pi y_n \cos 2\pi x_n. \tag{5}$$

An orbit is regarded as a cycle of period q if

$$x_{n+q}=x_n+p, \quad y_{n+q}=y_n, \tag{6}$$

where p is an integer. In Table I we summarize data from numerical calculations revealing a set of unstable complex cycles with periods given by Fibonacci numbers. Among the points of the periodic orbits for the presentation we have selected those that obey a scaling relation: The ratio of two subsequent complex numbers in the left column of the table converges fast to a real value $\alpha=-1.288\,57\ldots$.

The last column of Table I contains the Floquet eigenvalues, or multipliers, for the periodic orbits found. The multiplier is defined as a factor determining evolution of a small perturbation over one period T. For our one-dimensional complex map the value of θ_T is an analytic function of θ_0, and the multiplier may be evaluated simply as a derivative:

$$\partial\theta_T/\partial\theta_0=\partial x_T/\partial x_0+i\,\partial y_T/\partial x_0$$
$$=\prod_{n=0}^{n=T-1}[1-k\cos 2\pi(x_n+iy_n)]. \tag{7}$$

From Table I we observe that the multipliers of the cycles with Fibonacci periods tend to a certain complex value $\mu_+\approx 0.7421+2.5428i$.

It is worth mentioning that each member of the sequence of unstable cycles given in Table I has a complex conjugate partner. Hence, there exists a sequence of cycles with multipliers converging to a conjugate constant $\mu_-=\mu_+^*$. It may be conjectured that both these conjugate sets of periodic orbits are infinite.

III. RENORMALIZATION GROUP ANALYSIS

To explain the results of the previous section we employ the RG technique developed in [4–6,19,20,28,29]. The main idea consists in considering a set of evolution operators that describe the dynamics at the critical point over increasing time intervals. For the case of the golden-mean winding number, these time intervals are selected as subsequent Fibonacci numbers F_m.

Let us introduce a shortened notation for the circle map,

$$\theta_{n+1}=f(\theta_n), \tag{8}$$

and consider the evolution of some initial θ_n over a time interval given by a Fibonacci number F_{m+1}. As the rational approximant of the winding number is F_m/F_{m+1}, we conclude that $\theta_{n+F_{m+1}}$ is close to F_m. We recall that only the fractional part of θ_n is relevant and represent the evolution operator over F_{m+1} iterations as

$$f_m(\theta)=f^{F_{m+1}}(\theta)-F_m$$
$$=\underbrace{f(f(f(\ldots(\theta)\ldots)))}_{(F_{m+1}\text{ times})}-F_m. \tag{9}$$

According to the Fibonacci relation $F_{m+1}=F_m+F_{m-1}$ we write

$$f_{m+1}(\theta)=f_{m-1}(f_m(\theta)). \tag{10}$$

[Note that for any integer p the function $f(\theta)$ obeys $f(\theta+p)=f(\theta)+p$.] Next, following Refs. [4–6], at each step m we implement rescaling of the dynamical variable by the factor α^m and rewrite Eq. (10) in terms of the renormalized evolution operators $g_m(\theta)\equiv\alpha^m f_m(\alpha^{-m}\theta)$:

$$g_{m+1}(\theta)=\alpha^2 g_{m-1}(\alpha^{-1}g_m(\alpha^{-1}\theta)). \tag{11}$$

This expression defines the RG transformation.

If the parameters of the original map correspond to the GM critical point, then the functional sequence $g_m(\theta)$ converges to a definite limit: $g(x)=\lim_{m\to\infty}g_m(x)$. The limit function $g(\theta)$ is the fixed point of the RG transformation (10) and, hence, must satisfy the functional equation of Feigenbaum-Kadanoff-Shenker:

$$g(\theta)=\alpha^2 g(\alpha^{-1} g(\alpha^{-1}\theta)). \tag{12}$$

This function represents a form of the long-time evolution operators in terms of the rescaled dynamical variable. It is convenient to accept normalization of $g(\theta)$ to unity at the origin. Then this function may be found directly from solution of Eq. (12) [4–6,28,29]. With the help of a finite polynomial approximation for $g(\theta)$ one can reduce the functional equation to a set of algebraic equations for the coefficients of the expansion, and solve them numerically by means of the multidimensional Newton method. We have reproduced these calculations and find the universal function

$$\begin{aligned} g(\theta)=1&+0.765\,184\theta^3-0.215\,464\theta^6-0.053\,469x^9\\ &+0.032\,921\theta^{12}+0.001\,231\theta^{15}-0.004\,304\theta^{18}\\ &+0.000\,668\theta^{21}+0.000\,501\theta^{24}+0.000\,177\theta^{27}\\ &-0.000\,042\theta^{30}+0.000\,031\theta^{33}-0.000\,004\theta^{39}\cdots \end{aligned} \tag{13}$$

and the constant $\alpha=-1.288\,574\,55\ldots$ in excellent agreement with Refs. [4–6,28,29]. Now we take an additional step and suppose that the variable θ is complex. Using Eq. (13) one can check that the universal function $g(\theta)$ has the following fixed point:

$$\theta_+=g(\theta_+),\ \theta_+=0.686\,628\ldots+i0.604\,309\ldots. \tag{14}$$

and the derivative at this point is

$$\mu_+=g'(\theta_+)=0.742\,130\,53\ldots+i2.542\,847\,59\ldots. \tag{15}$$

We recall that for large m the map $f_m(\theta)$, which describes the dynamics of the circle map at the GM critical point over F_{m+1} iterations, is represented by the function $g(\theta)$ up to normalization of the dynamical variable. Hence, each map $f_m(\theta)$ will have a complex fixed point, and this point corresponds to a complex cycle of period F_{m+1} for the original map. Starting points for these cycles behave as $\theta\propto\alpha^{-m}$, and multipliers given by the derivatives of $f_m(\theta)$ are equal asymptotically to the derivative of the universal function at the fixed point. This explains the results of the previous section. From Table I we see that the empirically obtained multipliers agree with the value of derivative (15), and the ratio of starting coordinates for the complex periodic orbits coincides with the scaling constant (3).

The coefficients in formula (13) are real; hence, the fixed point θ_+ has a complex conjugate partner—the fixed point $\theta_-=\theta_+^*$ with the derivative $g'(\theta_-)=\mu_-=\mu_+^*$.

On the basis of the RG analysis we conclude that the existence of a set of unstable cycles, whose periods are given by Fibonacci numbers and whose multipliers converge to the universal constant, is an attribute of the universality class associated with the GM critical point, rather than a property of the concrete circle map. This circumstance can be exploited to search for the critical point in other systems, including invertible two-dimensional maps.

In the final part of this section we recall the results of analysis of perturbations for the fixed point of the Feigenbaum-Kadanoff-Shenker RG equation [4–6,19,20,28,29]. We search for a solution as $g_m(\theta)=g(\theta)+\varepsilon h_m(\theta)$ and, accounting for terms of the first order in ε, obtain

$$\begin{aligned} h_{m+1}(\theta)=&\alpha^2 g'(\alpha^{-1}g(\theta/\alpha))h_m(\theta/\alpha)\\ &+\alpha h_{m-1}(\alpha^{-1}g(\theta/\alpha)). \end{aligned} \tag{16}$$

The substitution $h_m(\theta)=\delta^m h(\theta)$ leads to the eigenproblem

$$\delta^2 h(x)=\delta\alpha^2 g'(\alpha^{-1}g(x/\alpha))h(x/\alpha)+\alpha h(\alpha^{-1}g(x/\alpha)). \tag{17}$$

Computations yield two essential eigenvectors with eigenvalues $\delta_1=-2.833\,61\ldots$ and $\delta_2=\alpha^2=1.660\,42\ldots$ [see Eq. (4)]. The first eigenfunction has a Taylor expansion of the form $h_1(\theta)=1+\Sigma h_n\theta^{3n}$. In the circle map it corresponds to a perturbation preserving the cubic inflection point (a shift along the line $k=1$). The second eigenfunction $h_2(\theta)$ contains all powers of the argument. This perturbation appears due to a departure from the critical point along the curve of constant winding number. A general arbitrary shift of parameters from the GM critical point gives rise to both eigenvectors. In this case the evolution operators over time intervals F_m will behave asymptotically as

$$g_m(x)\cong g(x)+C_1\delta_1^m h_1(x)+C_2\delta_2^m h_2(x). \tag{18}$$

Here the coefficients C_1 and C_2 depend on the parameters of the original map and vanish at the critical point.

Suppose we consider the dynamics at some point of the parameter space (k,Ω), where the coefficients in Eq. (18) are C_1 and C_2. If we find another point (k',Ω') at which the coefficients are $C_1'=C_1/\delta_1$, $C_2'=C_2/\delta_2$, then the evolution operator, corresponding to F_{m+1} iterations at the new point, coincides with the operator for F_m iterations at the old point. Hence, at both these points the type of dynamics (periodic, quasiperiodic, chaotic) will be the same. The regimes differ only by the characteristic time scale: at the point (k',Ω') it is larger by the factor F_{m+1}/F_m, which tends to ω^{-1} as $m\to\infty$. All quantitative characteristics of the two regimes are expressed one via another by more or less trivial relations. For instance, the Lyapunov exponents are connected as

$$\Lambda(k',\Omega')\cong\omega\Lambda(k,\Omega). \tag{19}$$

The closer to the critical point, the more precise are the scaling relations.

IV. GM CRITICAL POINT IN THE STANDARD DISSIPATIVE MAP OF ZASLAVSKY

In this section we formulate a method for accurate computation of parameter values corresponding to the critical point. As an example, we take a well-known two-dimensional map—the standard dissipative map of Zaslavsky [9,25,35]. The method we suggest may be applied

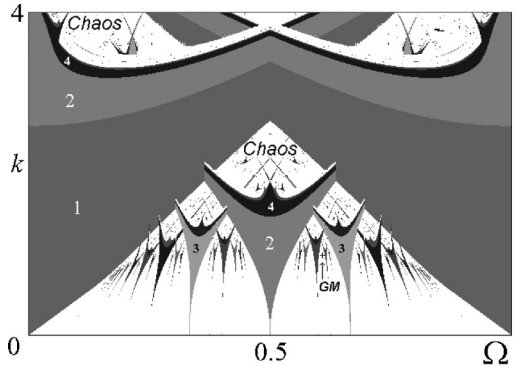

FIG. 2. Parameter plane of the dissipative Zaslavsky map (19). Regions of synchronization (Arnold tongues) are shown in gray; periods are indicated inside the tongues. White regions correspond to quasiperiodicity, chaos, or unrecognized long periods. The GM critical point found numerically is marked by a small cross.

also for a wide class of other maps and flows possessing the GM critical point.

The dissipative Zaslavsky map has been derived for some realistic physical systems and reads [9,25,35]

$$\theta_{n+1}=\theta_n+\Omega-(k/2\pi)\sin 2\pi\theta_n+dr_n,$$

$$r_{n+1}=dr_n-(k/2\pi)\sin 2\pi\theta_n, \tag{20}$$

where θ and r are dynamical variables, and Ω, k, d are parameters. For $d=0$ the map reduces to the circle map (1). So Ω and k have essentially the same nature as in the circle map, while the third parameter d is responsible for adding the second dimension. As in the circle map, the variable θ has the sense of a phase, so only periodic functions of θ may have a physical meaning.

It can be found that the Jacobi determinant of the map is constant and equal to d. The map is invertible: θ_n and r_n are expressed uniquely via θ_{n+1} and r_{n+1}. The Zaslavsky map may be regarded as a Poincaré map for some three-dimensional flow.

In Fig. 2 the chart of dynamical regimes in the parameter plane (Ω,k) is shown for fixed $d=0.3$. Periodic behavior is observed inside the Arnold tongues. While the parameter k is not large, quasiperiodicity occurs between the tongues. Chaotic regimes take place for larger k, in the upper part of the diagram. We assume that a GM critical point of the same universality class as in the circle map exists in the parameter plane. Certainly, it must belong to the curve of constant winding number $w=\lim_{n\to\infty}\theta_n/n=\omega=(\sqrt{5}-1)/2$. However, the map is invertible everywhere, and the criticality cannot be associated with violation of the invertibility. To invent an appropriate algorithm for computation of coordinates for the critical point we exploit the existence of a set of complex periodic orbits with the properties stated in Secs. II and III.

As the first step, let us extend the map into the complex domain. We assume that both dynamical variables in Eq. (20) are complex, $\theta=x+iy$, $r=u+iv$, while the parameters k,Ω,d remain real. Then, instead of Eq. (20), we write

TABLE II. Subsequent approximations for the GM critical point in the Zaslavsky map at $d=0.3$ found from the condition $S_{F_m}=\mu_+=0.742\,130\,53+2.542\,847\,59i$.

Period of complex orbit F_m	k	Ω
8	0.969272363707	0.610494183322
13	0.987131540725	0.610154623294
21	0.986520082743	0.610155713052
34	0.985390987646	0.610175758867
55	0.984925711397	0.610181199215
89	0.984745232773	0.610183894787
144	0.984693619730	0.610184570378
233	0.984676474491	0.610184812937
377	0.984672128558	0.610184871753
610	0.984670736356	0.610184891090
987	0.984670412056	0.610184895527
1597	0.984670306523	0.610184896984
2584	0.984670284034	0.610184897293

$$x_{n+1}=x_n+\Omega-(k/2\pi)\cosh 2\pi y_n\sin 2\pi x_n+du_n,$$

$$y_{n+1}=y_n-(k/2\pi)\sinh 2\pi y_n\cos 2\pi x_n+dv_n, \tag{21}$$

$$u_{n+1}=du_n-(k/2\pi)\cosh 2\pi y_n\sin 2\pi x_n,$$

$$v_{n+1}=dv_n-(k/2\pi)\sinh 2\pi y_n\cos 2\pi x_n.$$

If we have a cycle of period T starting at the point (θ_0,r_0), then

$$\theta_T=\theta_0+p,\quad r_T=r_0(p\text{ real integer}), \tag{22}$$

and two complex multipliers may be calculated as eigenvalues of the Jacobi matrix

$$\begin{pmatrix}\partial\theta_T/\partial\theta_0 & \partial\theta_T/\partial r_0\\ \partial r_T/\partial\theta_0 & \partial r_T/\partial r_0\end{pmatrix}$$

$$=\begin{pmatrix}\partial x_T/\partial x_0+i\partial y_T/\partial x_0 & \partial x_T/\partial u_0+i\partial y_T/\partial u_0\\ \partial u_T/\partial x_0+i\partial v_T/\partial x_0 & \partial u_T/\partial u_0+i\partial v_T/\partial u_0\end{pmatrix}. \tag{23}$$

The determinant of this matrix equals d^T, where $d<1$. For large T the determinant becomes very small in modulus, so one multiplier appears to be approximately zero, and the other is given by the trace of the matrix:

$$\mu_T\cong S_T=\partial x_T/\partial x_0+\partial u_T/\partial u_0+i(\partial y_T/\partial x_0+\partial v_T/\partial u_0). \tag{24}$$

Let us fix d and try to find values of k and Ω at which the map will have an infinite sequence of unstable complex cycles of periods given by Fibonacci numbers, and with trace asymptotically equal to the universal constant (15). These values of k and Ω will give an estimate for coordinates of the

TABLE III. Coordinates of GM critical point in dependence on the parameter d in the Zaslavsky map.

d	k_c	Ω_c
0.0	1.00000000000	0.606661063470
0.1	0.99349985654	0.608054206127
0.2	0.98856245192	0.609209827978
0.3	0.98467027409	0.610184897429
0.4	0.98149556207	0.611022944250
0.5	0.97883777906	0.611753902740

GM critical point: the larger the period, the more precise is the estimate. For a given Fibonacci number F_m we have to solve numerically the following set of six equations:

$$\begin{aligned} x_{F_m}(x_0,y_0,u_0,v_0,k,\Omega)-F_{m-1}&=x_0,\\ y_{F_m}(x_0,y_0,u_0,v_0,k,\Omega)&=y_0,\\ u_{F_m}(x_0,y_0,u_0,v_0,k,\Omega)&=u_0,\\ v_{F_m}(x_0,y_0,u_0,v_0,k,\Omega)&=v_0,\\ (\partial x_{F_m}/\partial x_0+\partial u_{F_m}/\partial u_0)&=\mathrm{Re}\,\mu_+,\\ (\partial y_{F_m}/\partial x_0+\partial v_{F_m}/\partial u_0)&=\mathrm{Im}\,\mu_+ \end{aligned} \tag{25}$$

to find six unknowns k, Ω, x_0, y_0, u_0, v_0. This may be done by means of the multidimensional Newton method. The crucial condition of success is to have an appropriate initial approximation for the solution. For cycles of moderate periods we can start from $d=0$, with the known data for the circle map, and then trace the solution for gradually increasing d up to a desirable value. For larger periods F_m another hint is possible: we can use data for previous periods to guess an initial approximation by means of scaling relations; see the discussion in Sec. V. The results of computations for one particular value $d=0.3$ are summarized in Table II. The parameter values clearly demonstrate convergence to a definite limit, which is the GM critical point for the Zaslavsky map. To find this point with high precision we have produced computations using 60-digit arithmetic and Fibonacci numbers such as 463 68 and 750 25. This yields

$$\begin{aligned} k_c&=0.984\,670\,284\,088\ldots,\\ \Omega_c&=0.610\,184\,897\,296\,4\ldots. \end{aligned} \tag{26}$$

In Fig. 2 this point is marked by a small cross.

In three-dimensional parameter space (Ω,k,d) there exists a curve consisting of the GM critical points. In Table III we present their coordinates for different values of d. Note that for $d=0.5$ our data are in excellent agreement with those of Ketoja [25].

V. SCALING PROPERTIES OF DYNAMICS AT THE GM CRITICAL POINT

In Table IV we present numerical data for the complex orbits of periods given by the Fibonacci numbers F_m from 8 to 1597 at the GM critical point. Observe that all the multipliers are approximately equal to the universal constant μ_+. It is possible to select one point at each orbit to ensure that the ratios $(\theta_{m-1}-\theta_{m-2})/(\theta_m-\theta_{m-1})$ and $(r_{m-1}-r_{m-2})/(r_m-r_{m-1})$ converge to the universal constant $\alpha=-1.288\,57\ldots$ (see the second and third columns of Table IV). These points tend to a definite limit as

$$\theta_{F_m}\cong\theta_c+K_1\alpha^{-m},\quad r_{F_m}\cong r_c+K_2\alpha^{-m}, \tag{27}$$

where K_1 and K_2 are some complex constants and

$$\theta_c=-0.001\,066\,68\ldots,\quad r_c=-0.037\,163\,04\ldots \tag{28}$$

are found to be real. We will refer to the point (θ_c,r_c) as *the scaling center*. For the Zaslavsky map it plays the same role as the origin (inflection point) in the circle map.

TABLE IV. Starting points of complex cycles and their multipliers for the Zaslavsky map (19) at $k=0.984\,670\,284\,088$, $\Omega=0.610\,184\,897\,296\,5$, $d=0.3$.

Period	θ_0	r	μ
8	$-0.085918149-0.075798541i$	$-0.078783593-0.034202902i$	$0.749444+2.553330i$
13	$0.065134717+0.059523013i$	$-0.004659935+0.029736586i$	$0.737749+2.550092i$
21	$-0.052559880-0.045420212i$	$-0.062206782-0.021206600i$	$0.738585+2.542746i$
34	$0.038977024+0.035560632i$	$-0.017616701+0.017614769i$	$0.739674+2.543508i$
55	$-0.032147406-0.027340455i$	$-0.052250324-0.012991441i$	$0.740865+2.542425i$
89	$0.023077997+0.021339526i$	$-0.025407804+0.010498662i$	$0.741459+2.542905i$
144	$-0.019800186-0.016472154i$	$-0.046254429-0.007900734i$	$0.741822+2.542700i$
233	$0.013479388+0.012829262i$	$-0.030089641+0.006281747i$	$0.741978+2.542858i$
377	$-0.012352715-0.009925091i$	$-0.042640889-0.004785266i$	$0.742065+2.542807i$
610	$0.007694500+0.007719485i$	$-0.032905266+0.003768004i$	$0.742099+2.542852i$
987	$-0.007864730-0.005979666i$	$-0.040463161-0.002891589i$	$0.742117+2.542837i$
1597	$0.004209845+0.004646827i$	$-0.034599563+0.002263721i$	$0.742124+2.542849i$
2584	$-0.005161120-0.003602216i$	$-0.039150975-0.001744938i$	$0.742128+2.542844i$

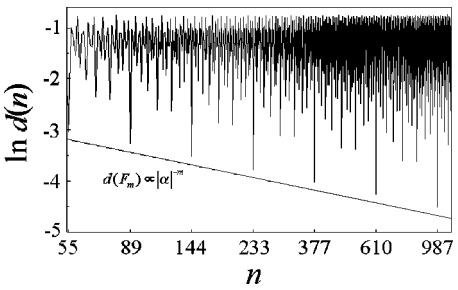

FIG. 3. Illustration of the scaling property for the orbit of the Zaslavsky map launched from the scaling center: dependence of the distance from the start point on the number of iterations. Double logarithmic scale is used.

To observe scaling in the dynamics of the Zaslavsky map in the real domain let us consider an orbit starting at the scaling center. In Fig. 3 the distance of the orbit from the initial point is plotted on a double logarithmic scale. Observe that the orbit returns closer and closer to the scaling center after the periods given by Fibonacci numbers F_m, and the distances behave as $d_m \propto |\alpha|^{-m}$.

As we mentioned, only periodic functions of θ can have a physical meaning; such an appropriate variable is, for example, $s=\sin(2\pi\theta)$. In Fig. 4 we show the attractor of the Zaslavsky map at the GM critical point in the plane (s,r). The cross indicates the location of the scaling center. Although this critical attractor itself looks rather like a cross section of a smooth torus, it has, in fact, a fractal nature because of the distribution of invariant measure. To make it visible, we use in Fig. 4 gray scale coding, which represents the relative probabilities of visiting different parts of the attractor.

Figure 5 illustrates self-similarity intrinsic to the fractal distribution of the invariant measure on the critical attractor. The upper diagram is a plot of the cumulative distribution function in dependence on the phase variable θ. Let us take a fragment of the picture near the scaling center and consider it at several steps of subsequent magnification (the bottom row in Fig. 5). Each time we redefine the scale by a factor $\alpha=$

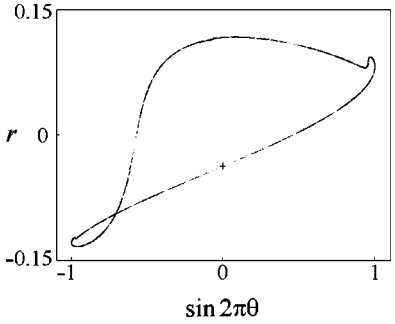

FIG. 4. Attractor of Zaslavsky map at the GM critical point drawn on the phase plane $(\sin 2\pi\theta, r)$. Gray scales code relative probabilities of visiting corresponding parts of the attractor. Note that the attractor itself looks like a cross section of a smooth torus. Its fractal properties are reflected only in the distribution of gray tones, representing structure of the invariant measure. The cross indicates location of the scaling center.

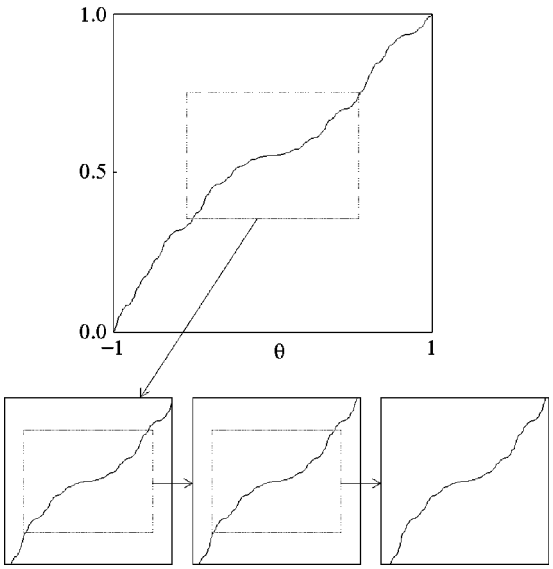

FIG. 5. Cumulative distribution function for invariant measure on the attractor at the GM critical point in the Zaslavsky map and illustration of its scaling property: a fragment of the whole picture is shown under subsequent magnification by factors $\alpha=-1.288\,57\ldots$ and $\beta=-(\sqrt{5}+1)/2$ along the horizontal and vertical axes, respectively.

$-1.288\,57\ldots$ along the horizontal axis, and by a factor $\beta=-(\sqrt{5}+1)/2$ along the vertical axis. (The minus sign means that the orientation of the axes is reversed at each subsequent step of the rescaling.) Observe that the pictures reproduce each other with good precision.

To reveal fractal properties of the invariant measure one can exploit the singularity spectrum introduced by Halsey *et al.* [39]. We have considered a sequence (θ_n, r_n) generated by the Zaslavsky map starting from the scaling center up to the iteration number $n=F_{m+2}=2584$ and define the diameters of covering elements as $l_i=\sqrt{\Delta\theta_i^2+\Delta r_i^2}$, where $\Delta\theta_i=(\theta_i-\theta_{i+F_{m+1}})/2\pi(\mathrm{mod}\,1)$, $\Delta r_i=r_i-r_{i+F_{m+1}}$, and their probabilities as $p_i=p=1/F_m$ for $i=1\ldots,F_m$. Next, we construct the sums

$$\Gamma_{q\tau}^{(m)}=\sum_{i=1}^{F_m} p^q/l_i^\tau=F_m^{-q}\sum_{i=1}^{F_m} l_i^{-\tau}, \tag{29}$$

consider their dependence on m, and require them neither to vanish nor to go to infinity. This yields

$$q(\tau)=\lim_{m\to\infty}\frac{\log\Gamma_{q\tau}^{(m)}}{\log F_m}\approx\frac{\log\Gamma_{q\tau}^{(m)}}{\log F_m} \tag{30}$$

for sufficiently large m. Then we define $\alpha=(dq/d\tau)^{-1}$ and $f=\alpha q-\tau$, and draw the parametric plot of $f(\alpha)$.

In Fig. 6 the singularity spectrum for the circle map at the GM critical point is shown by the solid curve, and the dots correspond to the singularity spectrum of the Zaslavsky map. The excellent coincidence of the spectra gives evidence that the critical points in both maps relate to the same class of universality. Generalized dimensions D_q may be calculated

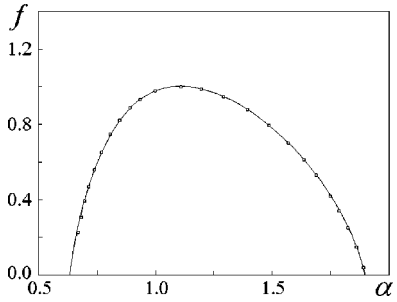

FIG. 6. Plot of the singularity spectrum for the attractor at the GM critical point: solid line corresponds to circle map, squares to the dissipative map of Zaslavsky.

from $D_{q(\tau)}=\tau/[q(\tau)-1]$. The Hausdorff dimension of the critical attractor is equal to 1, although the information and correlation dimensions have nontrivial values $D_1\cong 0.922$ and $D_q\cong 0.866$, the same for the circle map and the Zaslavsky map.

Let us turn to discussion of the Fourier spectrum generated by the Zaslavsky map at the GM critical point. Since only periodic functions of θ have physical meaning, we again introduce a variable $s_n=\sin 2\pi\theta_n=\sin 2\pi x_n \cosh 2\pi y_n + i\cos 2\pi x_n \sinh 2\pi y_n$, and will be interested in its Fourier expansion. We can arrive at the Fourier spectrum at the critical point by considering subsequent complex periodic orbits of period $N=F_m$ for larger and larger m. The spectral amplitudes are defined in the standard manner as

$$S(f)=S(m/N)=|c_m|^2,$$

$$c_m=\frac{1}{N}\sum_{n=0}^{N} s_n \exp[-(2\pi i m n)/N], \tag{31}$$

where $f=m/N$ is the frequency of the mth component. In Fig. 7(a) we present the spectrum obtained numerically at the GM critical point of the Zaslavsky map in the coordinates used usually in experimental studies: the logarithm of the amplitude versus frequency. To show the self-similar structure of the spectrum, we follow Refs. [3,6] and plot the spectrum on a double logarithmic scale. As observed in Fig. 7(b), the same arrangement of spectral peaks is reproduced with proper periodicity at intervals along the axis of logarithm of frequency.

VI. SCALING PROPERTIES OF THE PARAMETER PLANE IN THE VICINITY OF THE GM CRITICAL POINT

In this section we intend to demonstrate two-dimensional scaling of the parameter space near the GM critical point, which follows from the considerations in the last part of Sec. III. For this aim we need to define an appropriate local coordinate system (scaling coordinates) in such a way that simultaneous scale change along the coordinate axes by factors δ_1 and δ_2 would ensure realization of similar regimes. As we do not know explicit expressions for the coefficients in Eq. (18) via parameters of the model maps (1) and (20), the problem must be solved numerically, with sufficient accuracy.

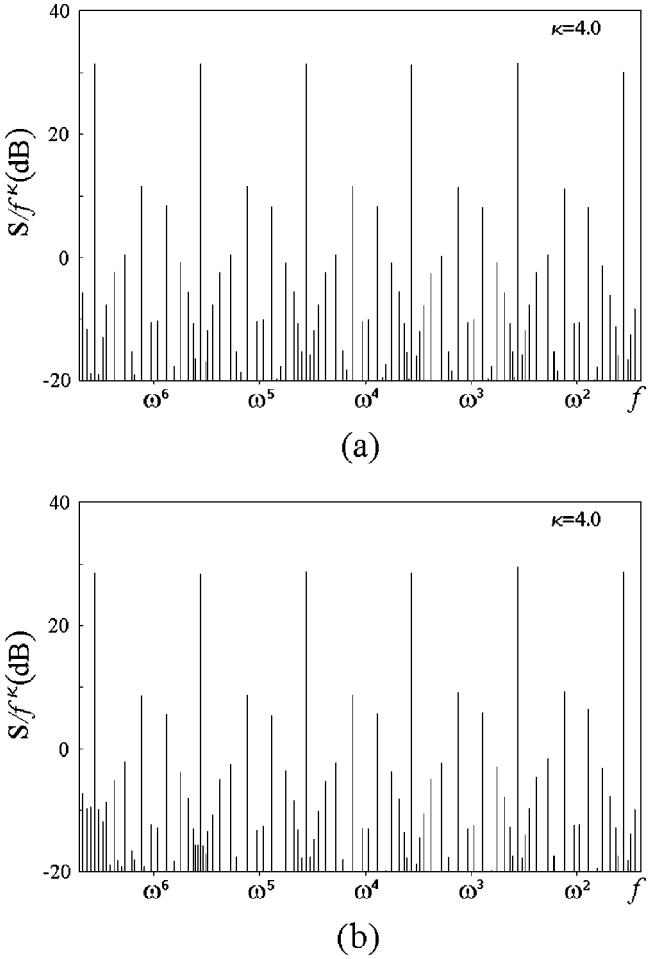

FIG. 7. Fourier spectra for time series generated by Zaslavsky map at the GM critical point (approximated by the cycle of period $F_1=2584$): (a) logarithmic plot for amplitude versus frequency; (b) double logarithmic plot; exponent k is fitted empirically.

Let us place the origin of the new coordinate system (c_1,c_2) at the GM critical point. Arbitrarily, we direct the first coordinate axis c_1 along the line $k=\text{const}$. In contrast, the second coordinate curve, along which the value of c_2 is measured, must be defined carefully to exclude a contribution of the senior eigenvector for any shift from the critical point along this curve (Fig. 8). It appears that it is just a curve of constant (golden mean) winding number. One could

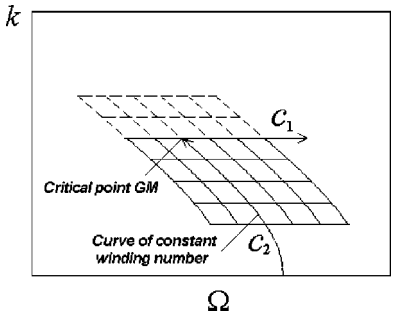

FIG. 8. Definition of scaling coordinates in the neighborhood of the GM critical point.

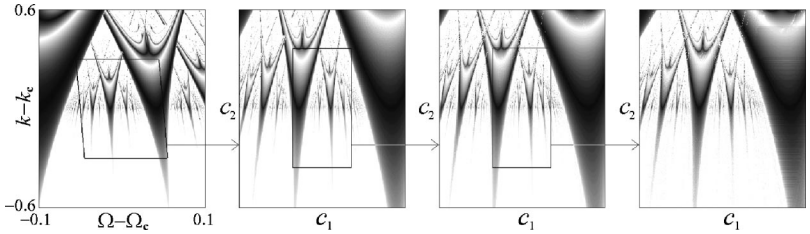

FIG. 9. Chart of Lyapunov exponent in the parameter plane of the circle map with fragments shown separately in scaling coordinates under subsequent magnification by factors δ_1 and δ_2 along the coordinate axes. Gray scales code values of the Lyapunov exponent Λ from $-\infty$ (light gray) to -0 (dark gray); zero and positive values are designated as white. For the pictures in scaling coordinates the coding rule is redefined in accordance with Eq. (19) at each subsequent step of magnification.

try to represent this curve by means of Taylor expansion $\Delta k = c_2$, $\Delta\Omega = Ac_2 + Bc_2^2 + Cc_2^3 + \cdots$. However, if we take into account the concrete relation between scaling factors δ_1 and δ_2, this expression may be cut. Indeed, suppose we consider a set of the parameter plane pictures under the scale change $c_1 \propto \delta_1^{-m}$ and $c_2 \propto \delta_2^{-m}$ for subsequent m. If we neglect the Taylor coefficient at c_2^j the deflection from the true coordinate curve will be of order δ_2^{-jm}, which yields a contribution to the senior eigenvector of order $\delta_2^{-jm}\delta_1^j$. As one can see from Eq. (4), the eigenvalues for the GM critical point satisfy $\delta_2 < |\delta_1|$, $\delta_2^2 < |\delta_1|$, but $\delta_2^3 > |\delta_1|$. Hence, it is necessary to account for only linear and quadratic terms in the Taylor expansion. So we may approximate the curve of constant winding number by a parabola and define scaling coordinates near the GM critical point by the ansatz

$$\Omega = \Omega_c + c_1 + Ac_2 + Bc_2^2, \quad k = k_c + c_2, \tag{32}$$

which is appropriate for both the circle map and the Zaslavsky map. As we have found numerically, for the circle map

$$A = -0.017\,49, \quad B = -0.001\,48, \tag{33}$$

and for the Zaslavsky map at $d = 0.3$

$$A = -0.013\,796, \quad B = -0.004\,543. \tag{34}$$

In Figs. 9 and 10 we demonstrate scaling of the parameter plane topography for both maps near their GM critical points. Gray tones code values of the Lyapunov exponent. In both cases the first plot shows a part of the parameter plane in ''natural'' coordinates (k,Ω). We then select a fragment of the picture near the GM critical point with the borders going along the coordinate curves $c_1 = \text{const}$ and $c_2 = \text{const}$, and redraw this fragment separately in scaling coordinates. Then the smaller fragment of the picture is magnified by factors δ_1 and δ_2 along the horizontal and vertical axes, respectively, and the gray scale coding is redefined in accordance with Eq. (18). This procedure of rescaling may be repeated again and again. Observe the excellent correspondence of the structures on different scales. The deeper the level of resolution, the better the correspondence between the pictures.

VII. CONCLUSION

The results of this paper should be regarded in the context of research directions that deal with the study and classification of critical behavior at the border of chaos. We mean situations associated with various classes of quantitative universality, allowing description in terms of the renormalization group approach [33]. When some different type of criticality is discovered in a simple artificial model, the question of the possibility of its observation in realistic dynamical systems immediately arises. Examples of such systems should be presented with a convincing demonstration of the corresponding dynamical properties in numerics and experiments.

Although the critical situation associated with destruction of the golden-mean two-frequency quasiperiodicity and the GM critical point has been known for about 20 years, the details are not complete yet. In this article we have found an interesting property of the critical dynamics associated with the GM point. That is, an infinite set of Fibonacci-period unstable orbits occurs in the complex domain of dynamical

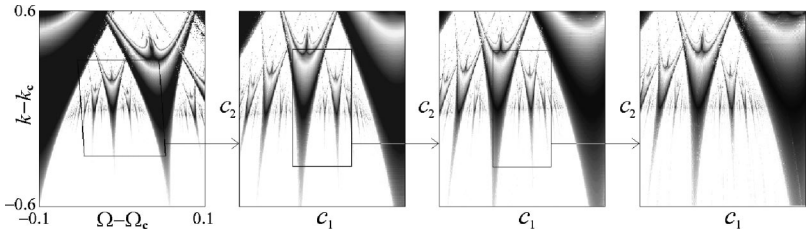

FIG. 10. Chart of Lyapunov exponent in the parameter plane of the Zaslavsky map for $d = 0.3$ with fragments shown separately in scaling coordinates under subsequent magnification by factors δ_1 and δ_2 along the coordinate axes. Gray scales code values of the Lyapunov exponent Λ from $-\infty$ (light gray) to -0 (dark gray); zero and positive values are designated as white. For the pictures in scaling coordinates the coding rule is redefined in accordance with Eq. (19) at each subsequent step of magnification.

variables, and Floquet eigenvalues (multipliers) of these cycles converge fast to a universal complex constant. This result follows also from the RG analysis; hence, it has to be regarded as an attribute of the whole universality class, not of some particular model. The stated property may be useful for accurate numerical estimates of the critical point location in the parameter plane for dissipative systems defined analytically by maps or differential equations. We have presented the corresponding data relating to the standard dissipative map of Zaslavsky.

One more essential contribution of the present work we see in the accurate analysis of two-dimensional scaling of the configuration of Arnold tongues near the GM critical point. That is, to observe self-similarity of this two-dimensional picture it is necessary to use a special curvilinear coordinate system in the parameter plane. ''Natural'' parameters of the original map are connected with the new coordinates via a parameter change, in which linear and quadratic terms must be included.

A more or less straightforward perspective of further studies is the possibility of application of the suggested approach to other systems manifesting GM critical behavior, and the elaboration of analogous analysis for other cases of destruction of two-frequency quasiperiodicity, say, for frequency ratios associated with the silver mean and other irrationals. As a matter of principle, we stress the fact that analysis of dynamics in the complex domain (in our case, the study of complex periodic orbits) leads to useful conclusions about dynamics in the real domain: It gives a foundation for constructing algorithms and sheds light on properties of universality and scaling. Similar approaches based on complexification of the dynamical systems under study may be productive in other problems of nonlinear dynamics, in particular, for deeper understanding of the dynamics between order and chaos.

ACKNOWLEDGMENTS

We thank Ulrike Feudel, Arkady Pikovsky, and Michael Zaks, for discussion, Igor Sataev for help in numerical calculations, and Sang-Yoon Kim for useful comments. This work was supported by the Russian Foundation of Fundamental Research, Grant No. 00-02-17509. N.I. acknowledges support from CRDF via the Research Educational Center of Saratov University (Grant No. REC-006).

[1] L.D. Landau, Dokl. Akad. Nauk SSSR **44**, 339 (1944).
[2] D. Ruelle and F. Takens, Commun. Math. Phys. **20**, 167 (1971).
[3] S.J. Shenker, Physica D **5**, 405 (1982).
[4] M.J. Feigenbaum, L.P. Kadanoff, and S.J. Shenker, Physica D **5**, 370 (1982).
[5] D. Rand, S. Ostlund, J. Sethna, and E.D. Siggia, Phys. Rev. Lett. **49**, 132 (1982).
[6] D. Rand, S. Ostlund, J. Sethna, and E.D. Siggia, Physica D **8**, 303 (1983).
[7] M.H. Jensen, M.H. Bak, and T. Bohr, Phys. Rev. Lett. **50**, 1637 (1983).
[8] M.H. Jensen, M.H. Bak, and T. Bohr, Phys. Rev. A **30**, 1960 (1984).
[9] M.H. Jensen, M.H. Bak, and T. Bohr, Phys. Rev. A **30**, 1970 (1984).
[10] C. Grebogi, E. Ott, S. Pelikan, and J.A. Yorke, Physica D **13**, 261 (1984).
[11] K. Kaneko, Prog. Theor. Phys. **71**, 282 (1984).
[12] J.D. Farmer and I.I. Satija, Phys. Rev. A **31**, 3520 (1985).
[13] M.H. Jensen, L.P. Kadanoff, A. Libchaber, I. Procaccia, and J. Stavans, Phys. Rev. Lett. **55**, 2798 (1985).
[14] J. Stavans, F. Helsot, and A. Libchaber, Phys. Rev. Lett. **55**, 596 (1985).
[15] C. Grebogi, E. Ott, and J.A. Yorke, Physica D **15**, 354 (1985).
[16] R.E. Ecke, J.D. Farmer, and D.K. Umberger, Nonlinearity **2**, 175 (1989).
[17] X.-W. Wang, R. Mainieri, and J. Hlowenstein, Phys. Rev. A **40**, 5382 (1989).
[18] S. Kim, R.S. MacKay, and J. Guckenheimer, Nonlinearity **2**, 391 (1989).
[19] B. Fourcade and A.-M.S. Tremblay, J. Stat. Phys. **61**, 607 (1990).
[20] B. Fourcade and A.-M.S. Tremblay, J. Stat. Phys. **61**, 639 (1990).
[21] Guckenheimer J. Baesens, S. Kim, and R.S. MacKay, Physica D **49**, 387 (1991).
[22] D. Rockmore, R. Siegel, N. Tongring, and C. Tresser, Chaos **1**, 25 (1991).
[23] S.-Y. Kim and B. Hu, Phys. Rev. A **44**, 934 (1991).
[24] S.-Y. Kim, and D.-S. Lee, Phys. Rev. A **45**, 5480 (1992).
[25] J.A. Ketoja, Phys. Rev. Lett. **69**, 2180 (1992).
[26] V.W. Spinadel, Chaos, Solitons Fractals **8**, 1631 (1992).
[27] V. Baladi, D. Rockmore, N. Tongring, and C. Tresser, Nonlinearity **5**, 1111 (1992).
[28] T.W. Dixon, T. Gherghetta, and B.G. Kenny, Chaos **6**, 32 (1996).
[29] T.W. Dixon and B.G. Kenny, J. Math. Phys. **39**, 5952 (1998).
[30] M.J. Feigenbaum, J. Stat. Phys. **21**, 669 (1979).
[31] B. Derrida, A. Gervois, and Y. Pomeau, J. Phys. A **12**, 269 (1979).
[32] B. Hu and J.-M. Mao, Phys. Lett. **108A**, 305 (1985).
[33] A.P. Kuznetsov, S.P. Kuznetsov, and I.R. Sataev, Physica D **109**, 91 (1997).
[34] J.S. Bastos de Figueiredo and C.P. Malta, Int. J. Bifurcation Chaos Appl. Sci. Eng. **8**, 281 (1998).
[35] A. J. Lichtenberg and M. A. Lieberman (unpublished).
[36] S.J. Shenker and L.P. Kadanoff, J. Stat. Phys. **27**, 631 (1982).
[37] L.P. Kadanoff, Phys. Rev. Lett. **47**, 1641 (1981).
[38] R.S. MacKay, Physica D **7**, 283 (1983).
[39] T.S. Halsey, M.H. Jensen, L.P. Kadanoff, I. Procaccia, and B.I. Shraiman, Phys. Rev. A **33**, 1141 (1986).